# Chapter 2

## Electrical impedance applied to Hemodialysis and Peritoneal Dialysis

### 2.1 Whole body and segmental measurements

Two clinical methods of bioimpedance have been used in dialysis patients: 1) The standard distal BIA (Bioelectrical Impedance Analysis) or right-side bioimpedance configuration and, 2) segmental bioimpedance (SBIA). BIA views the body as one cylinder of a given length, (body height) and a constant cross-sectional area and therefore is prone to errors depending on body size and shape, and regional fluid accumulation. In SBIA each segment is mathematically treated as a separate cylinder and whole body composition is calculated as the sum of segments (Rosell et al 1997, Lozano et al 1995-a, 1995-b, 1994, 1992).

#### 2.1.1 Electrode positions

In Piccoli (2002-b) three alternative electrode position are shown: distal BIA, proximal BIA, and segmental BIA.

*Distal BIA.* The standard BIA, whole-body or right-side configuration is with the patient in supine decubitus position: Two electrodes (an injector I, and a sensor V) were dorsally placed on the right hand in the third metacarpo-phalangeal articulation and in the carpus, respectively. The pair on the foot was located in the third metatarso-phalangeal and in the articulation, figure 2.1 (Lukaski 1986, Kushner 1992). The standard reference is right emisoma, because in HD is free of vascular accesses. In this configuration, the total impedance of a subject with normal hydration is determined by 50% of the impedance of the inferior limbs, by 40% of the impedance of the superior limbs, and by 10% of the impedance of the trunk (Ellis KJ 2000, Foster KF et al 1996, Grimnes and Martinsen 2000, Houtkooper LB et al 1996, Lukaski HC 1996).

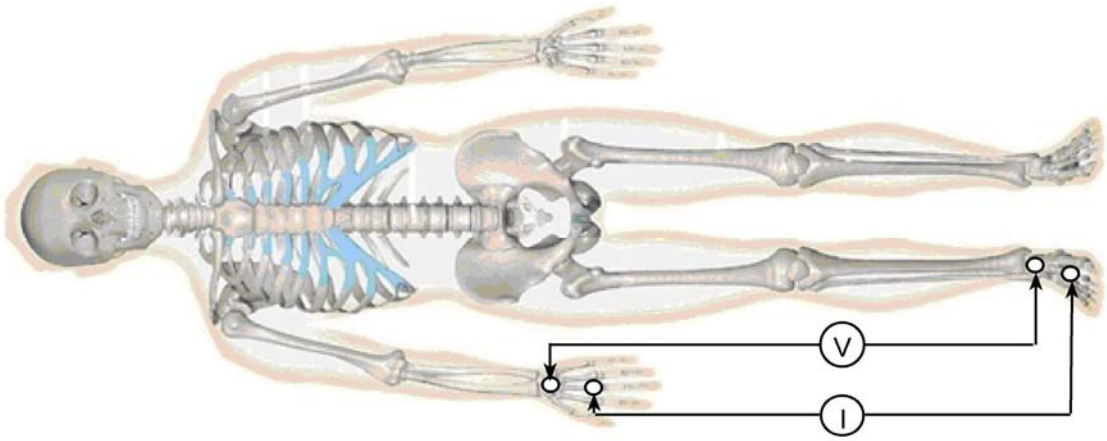


**Figure 2.1-** The standard electrode locations for BIA distal (right-side configuration)

*2. Proximal BIA.* In order to improve the estimation of the compartments of the conventional BIA, fluids and lean mass, different positions of cutaneous electrodes have been proposed (with the same basic model of cylindrical shape conductors and isotropy). Lukaski and Scheltinga (1994) proposed positions of the detector electrodes on the anterior-cubital fossa and in the popliteal fossa to obtain a proximal BIA, figure 2.2. The superiority of the proximal BIA is not yet demonstrated with respect to the distal in the estimation of the compartments in healthy adults, neither in a monofrequency nor multifrequency system (Lukaski HC et al 1994, Piccoli A et al 2002-a).

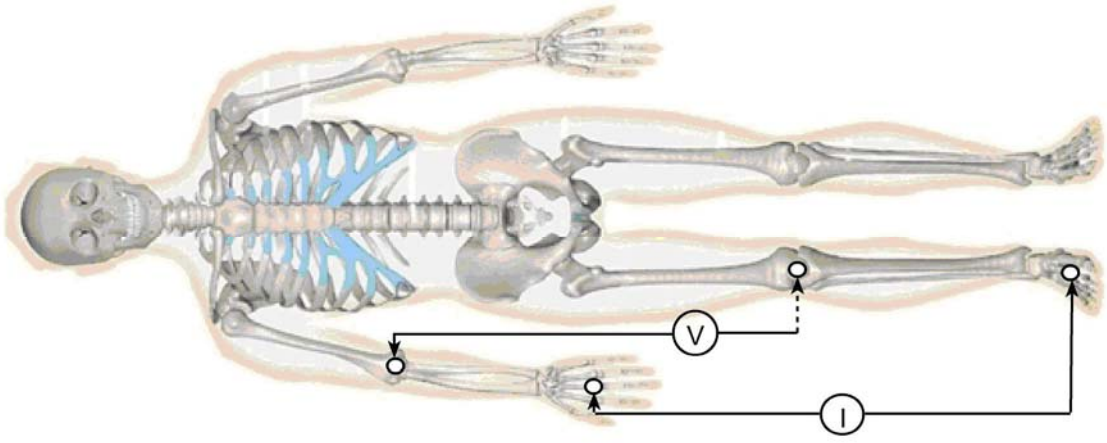


**Figure 2.2-** The electrode locations for BIA proximal (right-side configuration)

*3. Segmental BIA.* BIA segmental is obtained placing the electrodes at the end of the superior and inferior limbs, figure 2.3, and in the trunk, according to several modalities (Rosell et al 1997, Lozano et al 1995-a, 1995-b, 1994, 1992, Zhu et al 1998, 1999, Nescolarde et al 2004-

a, 2004-, 2004-c, Chanchairujira T et al 2001, Cornish BH et al 1993, 1999, Ellis KJ 2000, Foster KF et al 1996, Houtkooper LB et al 1996, Lukaski HC 1996, Chumlea et al 1988, Baumgartner et al 1989). The technique, nevertheless is still not standardized, and displays operative difficulties when identifying the reference points in the root of the members and on the trunk, mainly in oedema and obesity state. The reason of the failure is in discriminating different degrees from expansion of the fluids (Chanchairujira T et al 2001, Van Marken Lichtenbelt WD et al 1994).

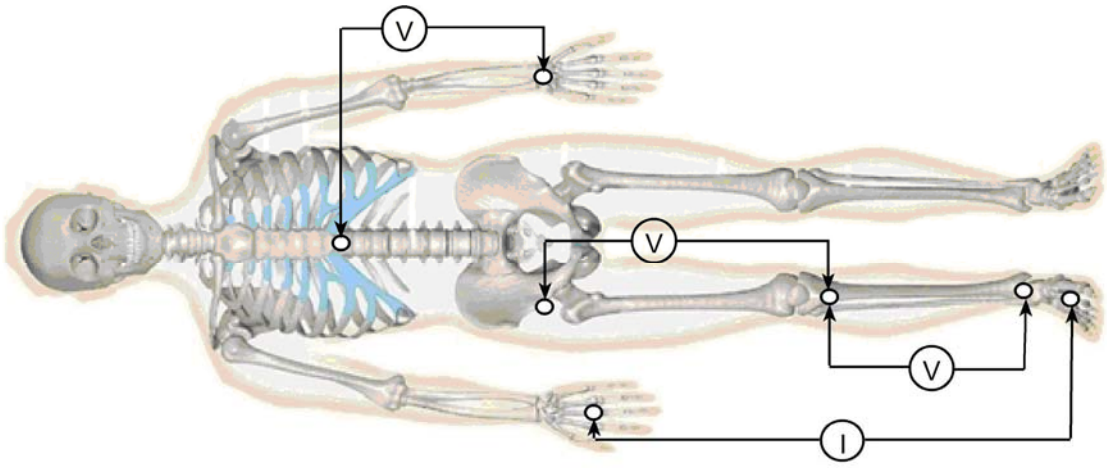


**Figure 2.3-** An example of electrode locations for BIA segmental

Distal BIA is the most widely used impedance technique in clinical application (Zhu et al 1999, Ellis 2000, Dilorio et al 2004, Kuhlman et al 2005), although in clinical setting, the standard method of right-side (Grimnes and Martinsen 2000) is not always applicable because a hand or a foot (right-side configuration) is not always accessible (Cox-Reijven et al 2002) or in other clinical situation as in peritoneal dialysis (PD) where each body segment of the CAPD patient has its own characteristic pattern of fluid shift in response to PD fluid exchange (Song et al 1999). In this case an alternative method would be helpful. Zhu et al 2000 and 2003 showed that segmental bioimpedance spectroscopy (SBIS) may be more accurate in measuring extracellular fluid (ECF) change than whole body bioimpedance spectroscopy (WBIS) in PD patients. However, Chanchairujira and Mehta (2001) evaluated both methods (SBIS and WBIS) in HD patients and conclude that both methods can be used to track relative ECF volume changes in HD; however, they found that are not accurate in quantifying change in absolute ECF volume.

## 2.2 Conventional bioelectrical impedance methods

### 2.2.1 Regression equations

The standard Bioelectrical Impedance Analysis (BIA) is measured between the right arm and the right leg, (whole body or righ-side impedance method) see figure 2.1. Based on this measurement body compartments (fat free mass, fat mass, extra and intra-cellular water, etc) are estimated using multiple regression equations (Table 2.1 and 2.2). These equations include one o more terms related to the measured impedance plus additional anthropometric terms (stature, weight, age, gender, etc). The measured electrical impedance term includes (Z) or its components, resistance (R) and reactance (Xc), in most of the cases, normalized by the height of the subject $H^2/R$. Usually R is measured at 50 kHz. Thre are equations to estimate volumes (intracellular, extracellular), masses (fat, fat-free, cellular), basal metabolism, and other variables (cellular Na/K, body density, etc). In general, these estimators are more susceptible to violating hypotheses, especially those regarding tissue hydration (Houtkooper et al 1996, Heymsfield et al 1997, Ellis 2000, Grimnes et al 2000, Piccoli et al 1994 and 2002). In such cases, the total body water (TBW) is estimated using the impedance component R and the FFM are estimated from the former by assuming a constant soft tissue hydration. The FAT mass is calculated as the difference between the FFM and the body weight (Foster et al 1996, Houtkooper et al 1996, Lukaski 1996, Heimsfield et al 1997, Ellis 2000). In most of the regression equations, the Xc component is ignored (Houtkooper et al 1996, Ellis 2000, Piccoli et al 2002). For the evaluation of malnutrition in HD patients, that is associated with greater morbidity and mortality, specific equations have been proposed to estimate the cellular mass (Chertow et al 1995).

**Table 2.1-**Examples of BIA equations derived for the prediction of TBW, ECW, and FFM (Ellis 2000)

| Age-Range | Number and Sex | Prediction Equation | SEE | Reference |
|---|---|---|---|---|
| *Single-frequency (50 kHz) BIA equations for TBW* | | | | |
| 4-7 days | 17 | 235.8 ($Wt \cdot Ht^2/R$) + 567 | 0.76 l | Mayfield and Waidelich 1999 |
| <3 yr | 65 | 0.67 ($Ht^2/Z$) + 0.48 | 0.36 l | Fjeld et al 1990 |
| 5-18 yr | 14F, 12M | 0.60 ($Ht^2/R$) - 0.50 | 1.69 l | Davies et al 1988 |
| 35-65 yr | 67F, 72M | 0.24 ($Ht^2/R$) + 0.172Wt + 0.165Ht + 0.039 ($Ht \cdot Wt$) — 17.577 | 3.47 l | Heitmann 1990 |
| 19-65 yr | 20F, 20M | 0.556 ($Ht^2/R$) + 0.096Wt + 1.73 | 1.75 l | Kushner and Schoeller 1986 |
| 19-42 yr | 37M | 0.63 ($Ht^2/R$) + 2.03 | 2.03 l | Lukaski et al 1985 |
| 20-73 yr | 28F, 25M | 0.372 ($Ht^2/R$) + 3.05 (sex) + 0.142Wt - 0.069age | 1.61 l | Lukaski and Bolonchuk 1988 |
| 19-61 yr | 20F, 88M | 0.484 ($Ht^2/R$) + 0.1444Wt + 1.356S + 0.105Xc - 0.057age | 1.53 l | Zillikens and Conway 1991 |
| *Single-frequency (50 kHz) BIA equations for FFM* | | | | |
| 10-14 yr | 41F, 53M | 0.83 ($Ht^2/R$) + 4.43 | 2.60 kg | Houtkooper et al 1989 |
| 7-15 yr | 166 | 0.406 ($Ht^2/R$) + 0.36Wt + 5.58Ht + 0.56 (sex) - 6.48 | 1.68 kg | Deurenberg et al 1991 |
| 7-25 yr | 140M | 0.156 ($Ht^2/R$) + 0.646Wt + 0.475AC - 0.116LC - 0.375MX - 2.932 | 2.31 kg | Guo et al 1987 |
| 7-25 yr | 110F | 0.182 ($Ht^2/R$) + 0.682Wt - 0.185LC - 0.244T - 0.202SS + 4.338 | 2.23 kg | Guo et al 1987 |
| 17-59 yr | 41F, 34M | 0.363 ($Ht^2/R$) + 0.214Ht + 0.133Wt | 3.06 kg | Segal et al 1985 |
| 17-62 yr | 498F, 1069M | 0.0013$Ht^2$ - 0.044$R$ + 0.305Wt - 0.168age + 22.668 | 2.43 kg (F) 3.61 kg (M) | Segal et al 1988 |
| 18-50 yr | 67F, 84M | 0.756 ($Ht^2/R$) + 0.11Wt + 0.107Xc | 2.06 kg | Lukaski et al 1986 |
| 16-83 yr | 661 | 0.34($Ht^2/R$) + 15.34Ht + 0.273Wt + 4.56sex - 0.127age - 12.44 | 2.63 kg | Deurenberg et al 1991 |
| 65-83 yr | 37F, 35M | 0.36 ($Ht^2/R$) + 0.359Wt + 4.5sex - 0.20TC + 7.0 | 2.50 kg | Deurenberg et al 1990 |
| 65-94 yr | 63F, 35M | 0.28 ($Ht^2/R$) + 0.27Wt + 4.5sex + 0.31TC - 1.732 | 2.47 kg | Baumgartner et al 1991 |
| *Dual-frequency BIA equations for TBW and ECW* | | | | |
| 19-64 yr | 36M | TBW = 0.455 ($Ht^2/R_{100}$) + 0.14Wt + 3.43 | 2.64 kg | Segal et al 1991 |
| | | ECW = 0.284 ($Ht^2/R_5$) + 0.112Wt - 6.115 | 1.94 kg | |
| 19-65 yr | 20F, 40M | TBW = 0.297 ($Ht^2/R_{224}$) + 0.147Wt - 3.637sex + 14.017<br>ECW = 0.099 ($Ht^2/R_{224}$) + 0.093Wt - 1.396sex - 5.178 | 3.58 kg<br>1.06 kg | Vanloan and Mayclin 1992 |
| 19-52 yr | 27F, 33M | TBW = 0.483 ($Ht^2/Z_{100}$) + 8.4<br>ECW = 0.229 ($Ht^2/Z_1$) + 4.5 | 2.27 kg<br>1.14 kg | Deurenberg et al 1994 |

BIA, bioelectrical impedance analysis; TBW, total body water; ECW, extracellular water; FFM, fat-free mass; Ht, height; Wt, weight; $R$, resistance; $Z$, impedance; $X$, reactance; SEE, standard error of estimate.

**Table 2.2**- Equations for adults suggested by Houtkooper et al 1996 for they accuracy and validation with respect to gold standard (Piccoli et al 2002-c)

| | |
|---|---|
| *Kushner et al 1986* | TBW= 0.556 $H^2/R$ + 0.095 Wt + 1.726 |
| *Kushner et al 1992* | TBW= 0.590 $H^2/R$ + 0.065 Wt + 0.040 |
| *Lukaski et al 1988* | TBW= 0.377 $H^2/R$ + 0.140 Wt - 0.080 year + 2.90 gender + 4.65 |
| *Lukaski et al 1986* | FFM= 0.756 $H^2/R$ + 0.110 Wt + 0.107 Xc - 5.463 |
| *Gray et al 1989* | FFM= 0.00108 $H^2$ - 0.02090 R + 0.23199 Wt - 0.06777 year + 14.59753, Female |
| | FFM= 0.00132 $H^2$ - 0.04394 R + 0.30520 Wt - 0.16760 year + 22.66827, Male |
| *Heitman et al 1990* | FFM= 0.279 $H^2/R$ + 0.181 Wt + 0.231 H + 0.064 gender Wt- 0.0777 year - 14.94 |
| *Deurenberg 1991-b* | FFM=0.34 $10^4$ $H^2$(m)/R + 15.34 H - 0.273 Wt - 0.127 year + 4.56 gender - 12.44 |
| *Stolarczyk et al 1994* | FFM=0.001254 $H^2$ - 0.04904 R + 0.1555 Wt + 0.1417 Xc - 0.0833 year + 20.05 |

TBW= total body water, FFM= fat free mass, FM= fat mas
H= height, Wt= weight, R= Resistance, Xc= Reactance

## 2.2.2 Cole-Cole model

The application of multifrequency bioimpedance measurement techniques, is closely related with the interpretation of the representation of the Cole-Z empirical equation (Cole 1940), eq. 2.1. The fluid distribution in the human body could be estimated from the Wessel diagram also called Cole or Cole-Cole plot.

The objective of multifrequency methods is to estimate the TBW (ECW and ICW) through R at high frequency ($R_\infty$) and the ECW through R at low frequency ($R_0$). The hypothesis is that at low frequency the current travel through the extracellular space and at high frequency travel between all spaces: intracellular and extracellular (Grimnes & Martinsen 2000), see figure 2.4.

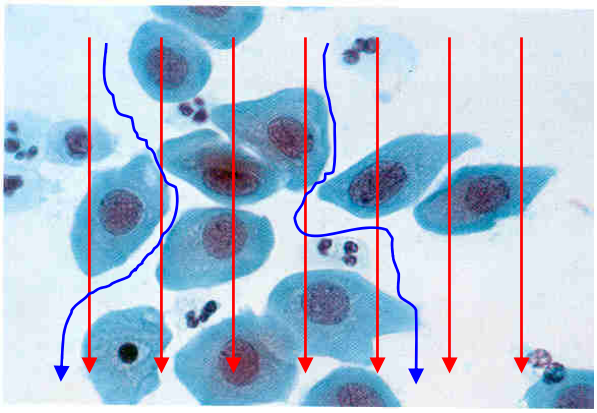

**Figure 2.4-** Current circulation in the biological tissue (→:high frequency, →: low frequency)

$$z = z_{\infty} + \frac{\left(r_o - r_{\infty}\right)}{1 + \left(j\omega\tau_z\right)^{\alpha}} \tag{2.1}$$

But, the Cole-Z equation commonly used is

$$Z = R_{\infty} + \frac{\left(R_o - R_{\infty}\right)}{1 + \left(j\omega\tau_z\right)^{\alpha}} \tag{2.2}$$

where

$\tau_z$ : Time Constant

α: Relaxation parameter (must be between 0 and 1)

The antecedents of the Cole-Z equation were found experimentally in Cole (1928-b) according with the theory summarized in Cole (1928-a). In this work, he presented the measuring cell and a tube oscillator, and the results obtained with a suspension of small eggs (Arbacia eggs). Cole (1932) repeated the representation from 1928 but together with an equivalent circuit with two static resistors and one constant phase element CPE, in series and parallel models, figure 2.5). The parallel model is best characterized by admittance, and the series model is best characterized by impedance; for these reason, the series model is used in conjunction with the Cole-Z equation (Grimnes and Martinsen 2000).

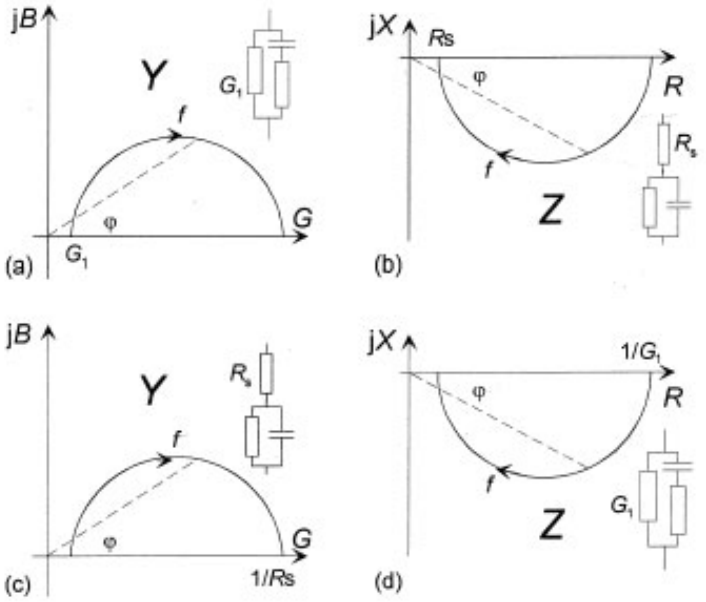


**Figure 2.5-** Wessel diagram of parallel and series equivalent circuit (Figure adapted from Grimnes and Martinsen 2000)

These spherical and isolated eggs, have been accepted successively as a good model for human cells, although the current distribution will completely different in a suspension of muscular fibers (Ellis 2000, Foster et al 1996, Grimnes, Martinsen 2000). The basic Cole impedance model describes only a single ideal dispersion. Often a biomaterial shows multiple dispersions (Grimnes and Martinsen 2000). Schwan in 1957 identified, for the fist time, three dispersions (α, β, γ) in the bioimpedance spectra (Figure 2.6):

1. The α-dispersion (mHz-kHz) whose mechanism is counterion effects (perpendicular or lateral) near the membrane zone, active cell membrane effects and gated channels, intracellular structures, ionic diffusion, dielectric losses.
2. The β-dispersion (0.1-100 MHz) whose mechanism is Maxwell-Wagner effects, passive cell membrane capacitance, intracellular organelle membrane, protein molecular response (structural membrane changes, hyper-hydration and oedema, and polarization of cell membrane).
3. The γ-dispersion (0.1-100 GHz) dipolar mechanism in polar media who reflect relaxation of water, and other small molecules such as salts and protein.

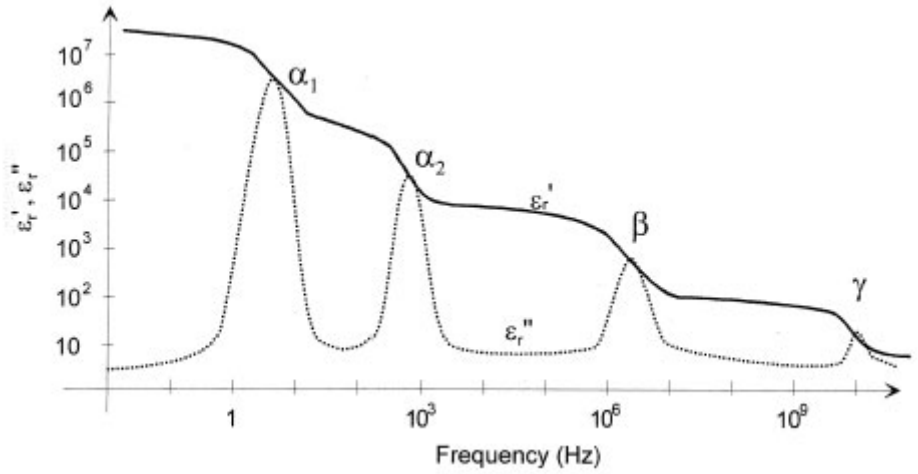


**Figure 2.6-** Dispersion region for biological tissue proposed by Schwan (1957) (Adapted from Grimnes and Martinsen 2000)

Unfortunately, when tissue hydration is variable, conventional BIA (at single frequency or multifrequency) produces inaccurate estimations for body compartments, as do other methods of body composition analysis (Abrahamsen et al 1996, Heymsfield et al 1997, Ellis 2000, Grimnes et al 2000). BIA can yield a fat mass increase in uremic obese patients at the end of an HD session. These results are the consequence of assuming constant hydration in soft tissues (which then indicates a FFM loss due to fluid elimination), and that FM is calculated as the difference between the FFM and the body weight (Piccoli et al 1998).

## 2.3 Bioelectrical Impedance Vector Analysis (BIVA)

In Piccoli et al (1994) the RXc-graph method was proposed. Resistance, R and reactance, Xc are obtained with right-side configuration in SFBIA at 50 kHz after standardization by height H. In contrast to other bioimpedance methods this approach does not yield any absolute estimate of ECW, ICW or TBW, makes no assumptions about body geometry, hydration state, or the electrical model of cell membranes and is unaffected by regression adjustments.

### 2.3.1 Descriptive statistics of impedance components

Without the need of an electric circuit model to represent and interpret the measurement results, Z can be considered as a bivariate random vector, with the same properties as either real or complex vector, (Letner 1982, Morrison 1967) representing a measurable property of soft tissues. The impedance vector is normalizate by the height of the subject (Z/H, Ohm/m). This is again assuming a cylindrical approximation of the body, where the measured impedance is proportional to the conductor length, and stature will be a surrogate for the conductor length of human body from hand to foot.

The intersubject variability of Z/H is appropriately represented with the bell-shaped bivariate normal distribution of the real R/H and imaginary Xc/H components of Z/H (Figure 2.7), Note, that the imaginary part is usually shown as a positive number when in fact is always negative for a biological tissue. The graph represents elliptical probability regions in the R/H-Xc/H plane with curves or surfaces showing the values of a probability function for the joint distribution of R/H and Xc/H values. We could plot in this graph the confidence ellipses for mean vectors and tolerance ellipses (Figure 2.8) for individual vectors (Piccoli et al 1994, 1995, 2002).

Bivariate Z-scores (Figure 2.8): after transformation of measured vector components of the RXc graph into bivariate Z-scores (Morrison 1967), i.e. R/H and Xc/H minus the mean and divided by the standard deviation of R/H and Xc/H calculated in the reference population. The RXc-score graph (Piccoli et al 2002-a) can be used with any analyzer in any population through its standard reference intervals.

### 2.3.2 Statistical inference with the RXc graph method

*Tolerance ellipses for individual impedance vectors.*

Three tolerance ellipses are considered in the RXc-graph, namely the median, the third quartile, and the 95th percentile, that are regions including 50%, 75% and 95% of individual points, respectively. These three tolerance ellipses allow a more detailed classification of vector position than the two (75% and 95%) that were used in the first article presenting the RXc graph method (Piccoli et al 1994).

By plotting the two components R/H and Xc/H measured in an individual subject as an individual impedance vector (a point) on the RXc graph, one can directly rank its distance from the reference mean vector through the tolerance ellipses (RXc point graph). Below, in the figure of BIVA patterns (figure 2.8), a seven-point scale is obtained considering upper and lower halves of tolerance ellipses larger than 50%.

The distance of the broken line connecting point vectors of repeated measurements in a same subject can also be ranked and compared with the reference, tolerance ellipses (RXc path graph).

*Confidence ellipses for mean vectors.*

By plotting the two mean components R/H and Xc/H measured in a group of subjects as a mean impedance vector with its 95% confidence ellipse, one can directly establish the mean vector position and variability in the corresponding population.

The sample mean is presented as estimator of results that would be obtained if the total population were studied. The lack of precision of a sample mean which results from both the degree of variability in the factor being investigated and the limited size of the study can be shown advantageously by a confidence interval.

*Comparison of mean vectors through confidence ellipses* (Jolicoeur 1995)

As with univariate analysis of continuous, normal variables, the confidence intervals show where mean are and can be utilized to test whether a mean is significantly different from some hypothesized value.

The inspection of a series of confidence intervals is very useful from a descriptive point of view and can help in interpreting statistical significance of tests (i.e. appreciating clinical

importance of "significant" differences). It is also the simplest way to rank the Mahalanobi's generalized distance (D) among mean vectors, which uses within-groups variation (elliptical shape) as a yardstick for differences between means (e.g. if D=4 between two vectors, then vectors differ by 4 within-groups variation). Multivariate statistical tests utilize functions of D.

As statistical tests of significance are related to confidence intervals of means, one can use confidence intervals for approximate comparison, of vector position of different populations.

In general, with unbalanced groups, if the 95% confidence intervals of each group means do not overlap, the group means are significantly ($P < 0.05$) different, but the reverse is not necessarily true. Indeed, there are situations where confidence intervals overlap only slightly, but the statistical test still declares a significant difference at the 5% level. This is due to the way of pooling group variances (assumed to be equal) in statistical tests and to the lower probability that two events occur jointly instead of separately. In comparison of means from two groups with a same sample size and a same variance, the graphic criterion using confidence ellipses is equivalent to the statistical test.

Hence, the graphic criterion based on confidence intervals is more conservative than statistical tests as it tends to declare not significant small differences between mean values with overlapping confidence intervals, meaning that mean vectors are very close and the statistical difference is not important.

However, the most efficient statistical approach for comparing two sample means is based on their difference, both in statistical tests and in graphic procedures. If the 95% confidence ellipse of mean vector difference does not cover the zero point, then the statistical test is significant at $P< 0.05$. If it covers the zero point, the statistical test is not significant.

*Statistical tests on multivariate mean vectors* (Letner 1982).
The two-sample Hotelling's T2 test is just a multivariate extension of the Student's t test for unpaired data in comparison of mean vectors, i.e. two or more variables, from two groups. It is more sensitive than the Student's t test performed on each variable and entails a smaller risk of erroneously rejecting the null hypothesis.

The paired one-sample Hotelling's T2 test is a multivariate extension of the Student's t test for paired data in comparison of mean difference vectors, i.e. the differences of two or more

variables considered two times in the same subjects. Both the two-sample and paired one-sample Hotelling's T2 tests are available in the BIVA confidence file (Mean graph, and Paired graph sheet, respectively). These tests are reasonably robust against departures from normality data.

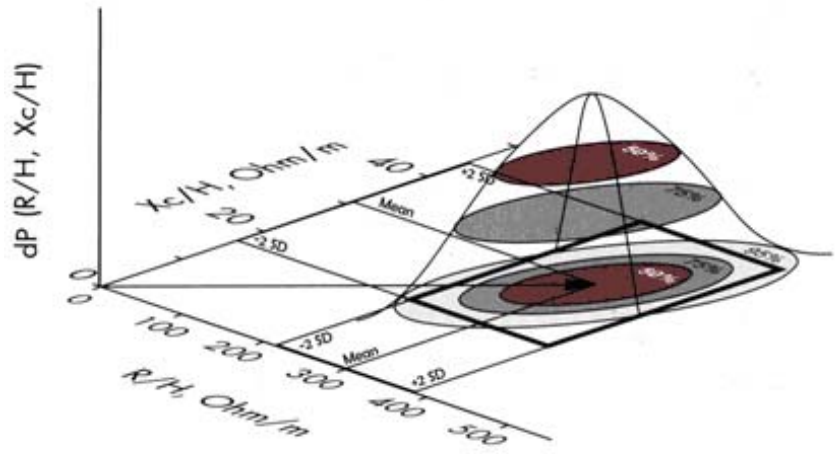


**Figure 2.7-**Univariate and bivariate the tolerance interval (Morrison 1967, Lentner 1982, Piccoli et al 1994)

Multivariate analysis of variance (MANOVA) is available in statistical software for comparisons of either mean vectors or mean difference vectors from more than two groups. Comparisons are made through multivariate tests like Wilk's lambda, Hotelling-Lawley trace, Pillai's trace, and Roy's maximum root which are transformed into F statistics for calculation of test probability and are equivalent to the Hotelling's T2 test in the comparison of two groups (BMDP, SAS, and SPSS software). As in univariate ANOVA, only approximate, complex procedures are available for multiple comparisons in MANOVA.

### 2.3.3 The RXc graph method in clinical bioimpedance analysis

The BIVA method is based on the measurement of the complex electrical impedance between the right hand and the right foot or whole-body (Grimnes & Martinsen 2000) with clinical application (Piccoli, et al. 1994, 1995, 1999, 1998, 2002-a, 2005-a, 2005-b)

*The RXc graph method makes three kinds of bioimpedance evaluation possible:*

*1)* Evaluation of a single vector measured the first time in an individual subject, plotting the point vector on the reference bivariate tolerance ellipses *(RXc point graph).*

2) Evaluation of patient's bioimpedance follow-up, plotting on the reference tolerance ellipses the broken line of random trajectory depicted by the successive measurements of the impedance vector in an individual patient *(RXc path graph).*

3) Evaluation of groups of subjects using the bivariate 95% confidence ellipses of the mean vectors (*RXc mean graph).* This is useful for clinical research studies aimed to identify disorders in body composition.

*Interpretation of individual vector position on the RXc graph*

Vector BIA with the RXc-graph method, allows an evaluation of soft tissues through patterns based on percentiles of their electrical properties without prior knowledge of body weight.

From clinical validation studies in adults, vectors falling out of the 75% tolerance ellipse indicate an abnormal tissue impedance, which is interpreted and ranked following the two directions of major and minor axis of tolerance ellipses:

1) Vector displacements parallel to the major axis of tolerance ellipses indicate progressive changes in tissue hydration (dehydration with long vectors, out of the upper pole, and hyperhydration with apparent oedema with short vectors, out of the lower pole).
2) Vectors falling (steady state) or migrating (dynamic state) parallel to the minor axis, above (left) or below (right) the major axis of tolerance ellipses indicate more or less cell mass, respectively, container in soft tissues, i.e. vectors with a comparable R value and a higher or lower Xc value, respectively.
3) Different trajectories indicate combined changes in both hydration and tissue mass.

Vector length is used as a proxy for volume state and increases during fluid removal with ultrafiltration. A shorter vector length at the start of hemodialysis suggests hyperhydration, especially when the vector is positioned outside the $75^{th}$ percentile of the norm and has been associated with increased mortality risk. Longer vectors, however, were not predictive of lower mortality risk (Piccoli et al 2004-b).

In a quite large fraction of patients, the vector point at the start as well as at the end of hemodialysis is located within the 75% distribution range of normal healthy adults, making it difficult to decide on the optimal post-hemodialysis weight in individual patients (Piccoli et al 1998, 2004-a).

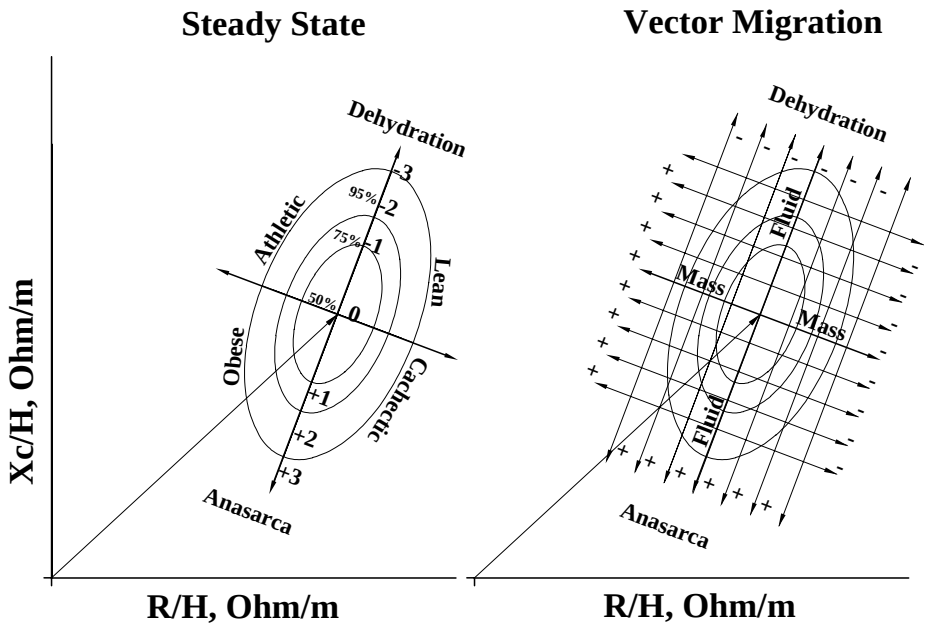


**Figure 2.8-** BIVA PATTERN (RXc-graph) (Piccoli et al 1994)

### 2.3.4 Formulas for calculation of confidence and tolerance ellipses

Geometrical parameters for drawing the RXc-graph and the RXc-score Graph in the case of bivariate normal distribution, confidence and tolerance intervals can be calculated by exact methods (Morrison 1967, Lentner 1982, Piccoli *et al* 1994, 1998, 2002).

After suitable modification of equations, common statistics of the simple linear correlation analysis can be used for calculation. Given $n$ pairs of observations $x$ and $y$, with SDs $s_x$ and $s_y$, and correlation coefficient $r$, for a fixed $\alpha$ probability level, take the Snedecor's $F_\alpha$ value with 2 and $n-2$ degrees of freedom.

In the RXc-graphs, the semiaxes $L_1$ and $L_2$, and the slopes b1 and $b_2=-1/b_1$ of the axes of the 100(1- $\alpha$) % confidence and tolerance ellipses ($\alpha$=0.05 $\alpha$=0.25 and $\alpha$=0.50; for the 95$^{th}$, 75$^{th}$ and 50$^{th}$ percentiles respectively) are calculated using equations

$$L_1, L_2 = \sqrt{K} * \sqrt{(n-1)(s_x^2 + s_y^2) \pm \sqrt{\left[(n-1)(s_x^2 + s_y^2)\right]^2 - 4(n-1)^2 (1-r^2)\, s_x^2 s_y^2}} \quad \text{and}$$

$$b_1, b_2 = \left(b, -1/b\right) = \frac{\left(s_y^2 - s_x^2\right)}{2rs_x s_y \pm \sqrt{1 + \left[\frac{\left(s_y^2 - s_x^2\right)}{2rs_x s_y}\right]^2}}.$$

In the RXc-score graph, parameters of tolerance ellipses of bivariate Z scores (RXc-score graph) can be calculated using equations $L_1, L_2 = \sqrt{K} * \sqrt{2(n-1) \pm 2r(n-1)}$ and $b_1, b_2 = \pm 1$

Where, $K = \frac{F}{n(n-2)}$, for confidence ellipses and $K = \frac{F(n+1)}{n(n-2)}$, for tolerance ellipses.

### 2.3.5 BIVA patterns from literature through the RXc-score graph

Data in the figure 2.9 are drawn from literature (Piccoli et al 2002) and plotted on the RXc-score graph after transformation of impedance measurements from several disease groups into bivariate Z-scores, with respect to their reference population. Solid and open circles represent male and female gender, respectively.

*Single score vectors* are from athletes, obese subjects of class I to III (Ob/1-3) or class I (Ob/1) [NHANES III population], patients with chronic renal failure (CRF) in conservative treatment, nephrotic syndrome (oedema), lung cancer, AIDS in stage WR 3-5 (HIV/3-5) or WR 6 (HIV/6), and anorexia nervosa.

*Repeated score vectors* are from climbers before and after high altitude dehydration, hemodialysis (HD) patients, either lean or obese (HDo) before and after fluid removal with a dialysis session, and dehydrated patients with cholera before and after fluid infusion.

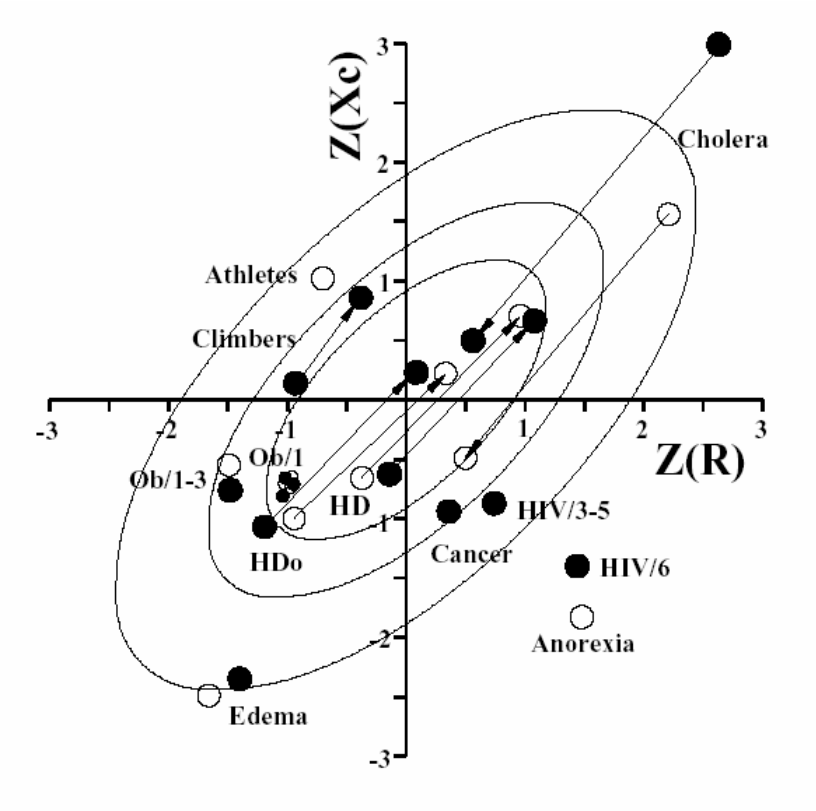


**Figure 2.9-** Z-score (Piccoli et al 2002)

**Adapted from:** Piccoli A, Pastori G: *BIVA software.* University of Padova, 2002 (E-mail: apiccoli@unipd.it).

## 2.4 References

Baumgartner RN, Chumlea WC, Roche AF (1989): Estimation of body composition from bioelectric impedance of body segments. *Am J Clin Nutr*, **50**:221-226

Cornish BH, Jacobs A, Thomas BJ, Ward LC (1999): Optimizing electrode sites for segmental bioimpedance measurements. *Physiol Meas*, **20**:241-250.

Cornish BH, Thomas BJ, Ward LC (1993): Improved prediction of extracellular and total body water using impedance loci generated by multiple frequency bioelectrical impedance analysis. *Phys Med Biol,* **38**:337.

Ellis KJ (2000): Human body composition: in vivo methods. *Physiol Rev*, **80**:649-680.

Foster KR, Schwan HP (1996): Dielectric properties of tissues. Handbook of Biological Effects of Electromagnetic Fields, Chapter 1; 25-103.

Grimnes S, Martinsen ØG (2000): *Bioimpedance and bioelectricity basics.* London, Academic Press.

Chanchairujira T, Metha RL (2001): Assessing fluid change in hemodialysis: Whole body versus sum of segmental bioimpedance spectroscopy. *Kidney Int*, **60**: 2337-2342.

Chumlea WC, Baumgartner RN, Roche AF (1988): Specific reistivity used to estimate fat-free mass from segmental body measures of bioelectrical impedance. *Am J Clin Nutr*, **48**:7-15

Hotelling H (1947): Multivariate Quality Control. In C. Eisenhart, M. W. Hastay, and W. A. Wallis, eds. Techniques of Statistical Analysis. New York: McGraw-Hill.

Houtkooper LB, Lohman TG, Going SB, Howell WH (1996): Why bioelectrical impedance analysis should be used for estimating adiposity. *Am J Clin Nutr,* **64**:436S-448S.

Jolicoeur P (1999): Introduction to biometry. New York, Kluwer Academic/Plenum Publisher

Kuhlmann MK, Zhu F, Seibert E, Levin NW (2005): Bioimpedance, dry weight and blood pressure control: new methods and consequences. Curr Opin Nephrol Hypertens, **14**:543-549

Lentner C (1982): Introduction to statistics. Statistical tables. Methematical formulae in Geigy Scientific Tables (vol 2, 8th ed), Basle, Ciba-Geigy Limited.

Lukaski HC (1996): Biological indexes considered in the derivation of the bioelectrical impedance analysis. *Am J Clin Nutr*, **64**:397S-404S.

Lukaski HC, Scheltinga RM (1994): Improved sensitivity of the tetrapolar bioelectrical impedance method to assess fluid status and body composition: use of proximal electrode placement. *Age Nutr*, **5**:123-129

Lukaski HC, Bolonchuck WW, Hall CB, Siders WA (1986): Validation of tetrapolar bioelectrical impedance method to assess human body composition. *J Appl Physiol*, **60**:1327-1332.

Lozano A, Rosell J and Pallàs-Areny R (1995): A Multifrequency multichannel electrical impedance data acquisition system for body fluid shift monitoring. *Physiol Meas*, **16**:227-237.

Lozano A, Rosell J, Riu PJ and Pallàs-Areny R (1995): Segmental body fluid shift estimation during HDT positions by electrical impedance measurements. Proceedings of the *IX International Conference on Electrical Bio-Impedance*. Heidelberg (Germany), 233-236.

Lozano A, Rosell J, Riu PJ and Pallàs-Areny R (1994): Multifrequency multisegment electrical impedance measurements for hemodialisis control. Proceedings of the *V International Symposium on*

*Biomedical Engineering*. Santiago de Compostela (España), 213-214.

Lozano A, Riu PJ, Rosell J and Pallàs-Areny R (1992): Multifrequency segmental electrical impedance measurements for body fluid shift determination. Proceedings of the *8th. International Conference on Electrical Bio-impedance*. Kuopio (Finland), 115-117.

Morrison DF (1967): Multivariate Statistical Methods. New York, MacGraw Hill.

Nescolarde L, Bragós R, Riu P, Doñate T, Rosell J (2004): Single-frequency multiple-segment impedance measurements in peritoneal dialysis. Proceedings of the *XII International Conference on Electrical Bioimpedance*. Gdansk (Poland). ISBN-83-917681-6-3, pp 263-266.

Nescolarde L, Bogónez P, Bragós R, Riu P, Doñate T, Rosell J (2004): Medidas segmentales-monofrecuencia en pacientes sujetos a diálisis peritoneal. Análisis del vector impedancia. Proceedings of the *XXII Congreso de la Sociedad Española de Ingeniería Biomédica CASEIB 2004*. Santiago de Compostela (España). ISBN 84-688-9318-8 pp 353-356.

Nescolarde L, Piccoli A, Núñez A, Román A, Doñate T, Rosell J (2004): Análisis del vector impedancia eléctrica en pacientes sujetos a diálisis: edema, mortalidad y medidas segmentales. Proceedings of the *IV Jornades de Recerca en Enginyeria Biomèdica*, Barcelona (España). ISBN 84-688-6747-0 pp 131-136.

Piccoli A, Pastori G (2002): *BIVA software.* University of Padova

Piccoli A, Pillon L, Dumler F (2002): Impedance vector distribution by sex, race, body mass index, and age in the United States: standard reference intervals as bivariate Z scores. *Nutrition,* **18**:153-167.

Piccoli A, Nescolarde L, Rosell J (2002): Análisis Convencional y Vectorial de Bioimpedancia en la Práctica Clínica. *Revista Española de Nefrología*, **XXII**: 230-240.

Piccoli A, Nigrelli S, Caberlotto A, Bottazzo S, Rossi B, Pillon L, Maggiore Q (1995): Bivariate normal values of the bioelectrical impedance vector in adult and elderly populations. *Am J Clin Nutr,* **61**:269-270.

Piccoli A, Rossi B, Pillon L, Bucciante G (1994): A new method for monitoring body fluid variation by bioimpedance analysis: The RXc graph. *Kidney Int,* **46**:534-539.

Rosell J, Casas O, Bragós R, Riu PJ and Andersen LJ (1997): Estimation of intra and extra-cellular segmental volumes using electrical impedance meaurements Proceedings of the World Congress on Medical Physics and Biomedical Engineering. Nice. ISSN:0140-018, pp 33

Snedecor, GW, Cochran WG (1989): Statistical Methods, Eighth Edition, Iowa State University Press.

Song JH, Lee SW, Kim GA and Kim MJ (1999): Measurement of fluid shift in CAPD patients using segmental bioelectrical impedance analysis. *Perit Dialysis Int*, **19**:386-390.

Sutcliffe JF (1996): A review of in vivo experimental methods to determine the composition of the human body. *Phys Med Biol,* **41**:781.

Winer BJ (1962): Statistical Principles in Experimental Design. New York: McGraw-Hill.

Zhu F, Hoenich NA, Kaysen G (2003): Measurement of intraperitoneal volume by segmental bioimpedance analysis during peritoneal dialysis. *Am J Kidney Diseases*, **42**:167-172

Zhu F, Schneditz D, Kaufman AM and Levin NW (2000): Estimation of body fluid changes during paritoneal dialysis by segmental bioimpedance analysis. *Kidney Int*, **57**: 299-306.

Zhu, F Schneditz D, Levin NW (1999): Sum of segmental bioimpedance analysis during ultrafiltration and hemodialysis reduces sensitivity to changes in body position. *Kidney Int* **56** (2):692-699.

Zhu, F Schneditz D, Wang E, Martin K (1998): Validation of changes in extracellular volume measured during hemodialysis using a segmental bioimpedance technique. *ASAIO J,* M541-M545